

# Momentum-inversion symmetry breaking on the Fermi surface of magnetic topological insulators

Hengxin Tan, Daniel Kaplan, and Binghai Yan

*Department of Condensed Matter Physics, Weizmann Institute of Science, Rehovot 7610001, Israel*

(Dated: May 17, 2022)

Magnetic topological insulators  $(\text{MnBi}_2\text{Te}_4)(\text{Bi}_2\text{Te}_3)_n$  were anticipated to exhibit magnetic energy gaps while recent spectroscopic studies did not observe them. Thus, magnetism on the surface is under debate. In this work, we propose another symmetry criterion to probe the surface magnetism. Because of both time-reversal symmetry-breaking and inversion symmetry-breaking, we demonstrate that the surface band structure violates momentum-inversion symmetry and leads to a three-fold rather than six-fold rotational symmetry on the Fermi surface if corresponding surface states couple strongly to the surface magnetism. Such a momentum-inversion symmetry violation is significant along the  $\Gamma - K$  direction for surface bands on the (0001) plane.

## I. INTRODUCTION

The intrinsic magnetic topological insulator  $\text{MnBi}_2\text{Te}_4$  and its sister compounds  $(\text{MnBi}_2\text{Te}_4)(\text{Bi}_2\text{Te}_3)_n$  ( $n = 0, 1, 2, 3$ ) [1–4] bring great opportunities for the realization of quantum anomalous Hall effect (QAHE) [5–8] and axion insulator (AI) [9–11]. Despite a magnetic surface gap being predicted in theory [12–17], most angle-resolved photoemission spectroscopy (ARPES) experiments, however, observed a gapless surface [17–27].

To address the discrepancy between experiment and theory, several candidate mechanisms based on either surface magnetic reconstruction, surface structural relaxation, or surface-bulk band hybridization have been proposed [15, 18, 20, 22, 28–34], among which the surface magnetic reconstruction is most extensively discussed. The ground state of bulk materials has the A-type anti-ferromagnetic configuration [intralayer ferromagnetic (FM) and interlayer anti-ferromagnetic (AFM)] for  $n = 0, 1, 2$  and FM configuration for  $n \geq 3$  due to the intensely weakening of the interlayer AFM super-exchange coupling [35–37]. The surface magnetism was anticipated to open an energy gap on the surface Dirac cone. Because most ARPES experiments observed no surface gap, it is speculated that the surface magnetic order may be changed to disorder, in-plane AFM (the magnetic moment is along the in-plane direction), or G-type AFM (*i.e.* AFM along all lattice vectors) (see, for example, Refs. 17, 18, and 22). However, recent spectroscopy experiments [38, 39] claimed that the bulk A-type AFM is robust on the surface. Thus, surface magnetism is still debated.

In this work, we propose to probe the surface magnetism via the symmetry of surface states besides searching for the magnetic gap. Because the magnetic surface naturally breaks the inversion symmetry and time-reversal symmetry ( $\mathcal{T}$ ), the surface band structure ubiquitously violates the momentum-inversion symmetry, for example, in the chiral surface Fermi arcs of a magnetic Weyl semimetal [40–42]. On the (0001) surface of these magnetic materials, we find that the Fermi surface exhibits a three-fold rotational symmetry if it cou-

ples strongly with the out-of-plane magnetism. Otherwise, the Fermi surface shows a six-fold rotational symmetry. In the surface Brillouin zone (BZ), such momentum-inversion symmetry breaking is significant along the  $\Gamma - K$  direction but vanishes along  $\Gamma - M$  due to symmetry constraint. We take  $\text{MnBi}_4\text{Te}_7$  ( $n = 1$ ) as an example to show the Fermi surface symmetry breaking on both  $\text{MnBi}_2\text{Te}_4$ - and  $\text{Bi}_2\text{Te}_3$ -terminated surfaces.

## II. METHOD

We performed density-functional theory (DFT) calculations with the plane-wave basis set, as implemented in Vienna *ab-initio* Simulation Package (VASP) [43, 44]. The cutoff energy for the plane-wave basis set is 350 eV. The generalized gradient approximation parameterized by Perdew-Burke-Ernzerhof [45] is used as the exchange-correlational functional between electrons. A Hubbard  $U$  of 5 eV is used for Mn- $d$  electrons. The bulk BZ is sampled by a  $k$ -grid of  $12 \times 12 \times 4$ . The zero damping DFT-D3 van der Waals correction [46] is included in all calculations. Spin-orbit coupling is considered in electronic structure calculations. The Wannier Hamiltonian is obtained by the maximally localized Wannier functions method [47] as implemented in WANNIER90 package [48] which is interfaced to VASP. The constant-energy contours (Fermi surfaces) of the surface states of  $\text{MnBi}_4\text{Te}_7$  (A-type AFM configuration) are calculated by a tight-binding scheme with thick slab models (more than 20 nm) [49] constructed from the bulk Wannier Hamiltonian. The surface states are identified by projecting wave functions to the top three surface van der Waals layers.

## III. RESULTS AND DISCUSSION

### A. Symmetry analysis of surface states

Let us start from the symmetry of a perfect (0001) surface without considering the magnetism (*i.e.*, paramagnetic case) in the first stage. The perfect (0001) surface

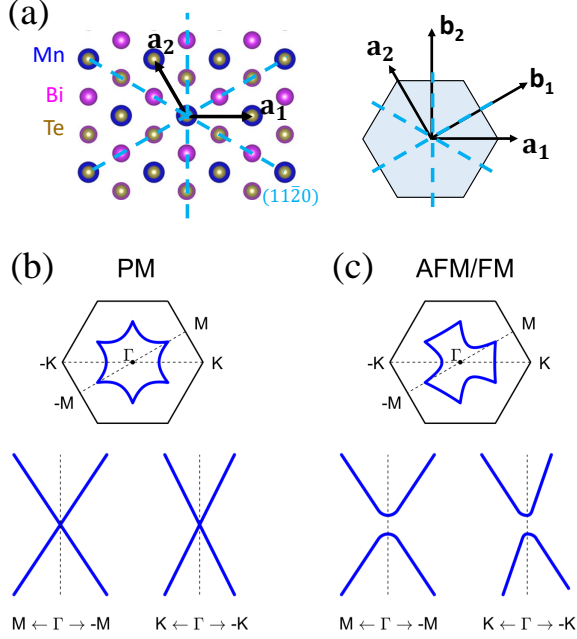


FIG. 1. Symmetry, schematic Fermi surface and surface states of the (0001) surface. (a) shows the top view of the MnBi<sub>2</sub>Te<sub>4</sub> surface structure (left panel) and the direction relationship between the lattice vectors  $\mathbf{a}_1/\mathbf{a}_2$ , reciprocal lattice vectors  $\mathbf{b}_1/\mathbf{b}_2$  and mirror planes in the first Brillouin zone (right panel). The cyan dashed lines represent three mirror planes projected onto the surface plane which are correlated by the three-fold rotational operation [the (1120) plane is labeled]. (b) shows the Fermi surfaces (upper) and surface states (lower) of the (0001) surface under the paramagnetic (PM) configuration, which have an equivalent  $C_{6v}$  symmetry. (c) is similar to (b) but for A-type antiferromagnetic/ferromagnetic (AFM/FM) case, where the Fermi surface has only equivalent  $C_{3v}$  symmetry with equivalent  $M$  and  $-M$  but non-equivalent  $K$  and  $-K$ . Notice that A-type AFM/FM also opens a band gap for the surface states in (c).

has  $C_{3v}$  symmetry which is generated by a three-fold rotational symmetry  $C_3$  around the out-of-plane axis and a mirror symmetry  $\mathcal{M}$  with respect to, e.g. the (1120) crystallographic plane as shown in Fig. 1(a). In the momentum space, the  $\Gamma-M$  line aligns inside the mirror plane. If  $\mathcal{T}$  is maintained, the band energy  $\varepsilon_n(\mathbf{k})$  is symmetric to  $\varepsilon_n(-\mathbf{k})$ . Combining  $C_3$  and  $\mathcal{M}$ , the band dispersion and the Fermi surface exhibit  $C_{6v}$  symmetry, as manifested schematically in Fig. 1(b).

Next we consider the A-type AFM where  $C_3$  holds. Time-reversal symmetry breaking eliminates the equivalence of  $\varepsilon_n(\mathbf{k})$  and  $\varepsilon_n(-\mathbf{k})$  at generic  $\mathbf{k}$  (e.g., along the  $\Gamma-K$  line). Thus, the  $C_{6v}$  symmetry of the Fermi surface is lifted. We note that a combined symmetry by  $\mathcal{M}$  and  $\mathcal{T}$  still preserves  $\varepsilon_n(\mathbf{k}) = \varepsilon_n(-\mathbf{k})$  along the  $\Gamma-M$  direction while it is asymmetric along  $\Gamma-K$  direction, as illustrated in Fig. 1(c). The combined  $\mathcal{MT}$  symmetry is equivalent to a new mirror reflection with respect to the  $\Gamma-K$  line in the Fermi surface. Together with  $C_3$ , the

Fermi surface exhibits  $C_{3v}$  symmetry.

As we mentioned above, some other magnetic configurations were also proposed, such as the in-plane AFM and G-type AFM [17, 18, 22]. For the same reason of  $\mathcal{T}$ -breaking, these cases also violate momentum-inversion symmetry on the Fermi surface, where  $C_3$  is further broken.

Besides the magnetic gap, we can monitor the surface magnetism by the  $C_{6v}$  symmetry-breaking of the Fermi surface. The magnitude of symmetry breaking indicates the coupling strength between topological surface states and surface magnetism. We stress that the momentum-inversion breaking is a general symmetry criterion and applies to general magnetic surface states. For example, the Fermi arcs reported in the recent magnetic Weyl semimetal Co<sub>3</sub>Sn<sub>2</sub>S<sub>2</sub> [40–42]) break the momentum-inversion symmetry [50]. However, such symmetry-breaking was rarely appreciated in recent studies on (MnBi<sub>2</sub>Te<sub>4</sub>)(Bi<sub>2</sub>Te<sub>3</sub>)<sub>n</sub>.

## B. Surface band structures

Taking MnBi<sub>4</sub>Te<sub>7</sub> as an example, we now demonstrate our symmetry analysis above by first-principles calculations with thick slab models under A-type AFM. The top and bottom surfaces of the slab are terminated by MnBi<sub>2</sub>Te<sub>4</sub> and Bi<sub>2</sub>Te<sub>3</sub> van der Waals layers, respectively. The interaction between top and bottom surfaces is avoided in the thick slab [49].

*MnBi<sub>2</sub>Te<sub>4</sub>-terminated surface.* The surface states of the MnBi<sub>2</sub>Te<sub>4</sub> surface of MnBi<sub>4</sub>Te<sub>7</sub> are shown in Fig. 2(a). The surface states near the Fermi energy open a magnetic gap (in the range of about 50 ~ 60 meV) which comes from the surface Dirac cone (located at the bulk band gap) due to the  $\mathcal{T}$ -symmetry breaking on the (0001) surface, consistent with previous theoretical calculations.

Figure 2(a) shows that the surface states along  $\Gamma-M$  line are symmetric while however, the surface states along the  $\Gamma-K$  line are asymmetric, consistent with our symmetry analysis in Sec. III A. We notice that the most prominent symmetry breaking happens on the top of the surface valence bands (in the energy range of  $-43 \sim -33$  meV relative to the maximum of the bulk valence bands), while the symmetry breaking at other energies is less apparent. In the energy range of  $-43 \sim -33$  meV, the surface valence bands are mainly contributed by the topmost MnBi<sub>2</sub>Te<sub>4</sub> layer and therefore couple strongly with magnetism. Fermi surfaces in Fig. 2(b) show more clearly the symmetry of surface states. For example, the constant-energy contour at  $-40$  meV shows clearly  $C_{3v}$  symmetry. Away from the top of the surface valence bands, Fermi surfaces display nearly  $C_{6v}$  symmetry because corresponding states are mainly contributed by the underlying Bi<sub>2</sub>Te<sub>3</sub> layer. For example, the  $C_{6v}$  is well preserved at  $\sim 0.3$  eV,

*Bi<sub>2</sub>Te<sub>3</sub>-terminated surface.* Similar symmetry breaking behaviors are also confirmed for the Bi<sub>2</sub>Te<sub>3</sub> surface

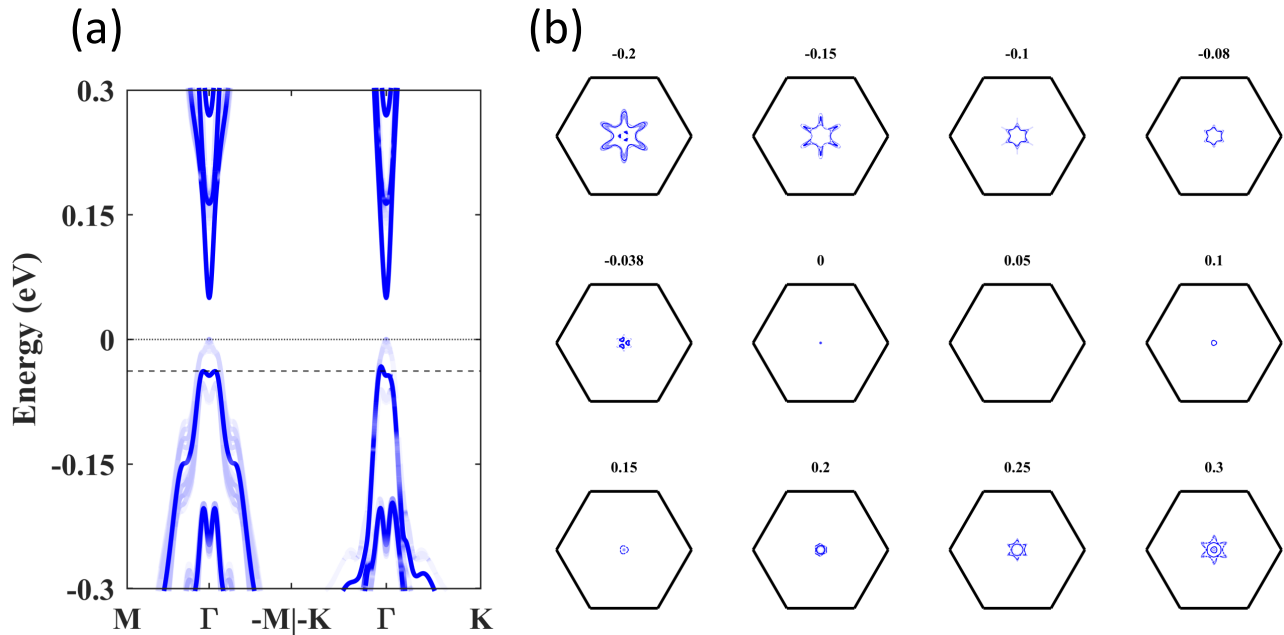


FIG. 2. Surface states and constant-energy contours of the  $\text{MnBi}_2\text{Te}_4$ -terminated surface of  $\text{MnBi}_4\text{Te}_7$ . (a) shows the surface states along  $\Gamma - M$  and  $\Gamma - K$  directions. The color blue stands for the weight of the surface (the larger the weight the darker the color). The surface states along  $\Gamma - M$  line are symmetric showing the “mirror symmetry”  $\mathcal{MT}$  while no such symmetry is shown along  $\Gamma - K$  line. (b) shows the constant-energy contours of the surface states in the full Brillouin zone (black hexagon) at different energies. The title of each panel shows the corresponding energy in eV. The surface states and constant-energy contours show that, while the  $C_{6v}$  symmetry is most obviously broken near the top of the surface valence bands ( $-0.038$  eV) as indicated by the dashed line in (a), the  $C_{6v}$  symmetry is well maintained at other energies *e.g.*, near the experiment Fermi level ( $\sim 0.3$  eV). Notice that the maximum of the bulk valence bands is set to energy zero.

as shown in Fig. 3. The most obvious symmetry breaking happens not only at the top of the surface valence bands (in the energy range of  $-49 \sim -35$  meV, relative to the bulk valence band maximum), but also at the energy range of  $-109 \sim -84$  meV, as indicated in Fig. 3(a). While the symmetry breaking surface state near  $-100$  meV is equally contributed by both the topmost  $\text{Bi}_2\text{Te}_3$  layer and  $\text{MnBi}_2\text{Te}_4$  layer beneath, the symmetry breaking branch near  $-40$  meV is solely contributed by the  $\text{MnBi}_2\text{Te}_4$  layer below the surface  $\text{Bi}_2\text{Te}_3$  layer. This is not strange because the magnetism comes from the Mn sublayer in the  $\text{MnBi}_2\text{Te}_4$  layer. The symmetry breaking of the surface band structures near these energies is more clearly shown in Fig. 3(b). In addition, the  $C_{6v}$  symmetry at other energies is well maintained. We note that the surface gap is filled with the bulk valence bands (filtered by the surface projection in Fig. 3) as discussed in the previous work [49].

We should point out that similar Fermi surfaces or band structures were also reported in recent calculations in the  $\text{MnBi}_2\text{Te}_4$ -family materials [4, 22, 24, 27]. However, the  $C_{6v}$ -breaking was rarely appreciated and discussed with respect to the interaction with surface magnetism.

#### IV. CONCLUSIONS

The momentum-inversion symmetry-breaking provides us a criterion to identify the surface magnetism besides

the surface magnetic gap. This symmetry criterion may be more accessible than the magnetic gap, especially when the long-sought magnetic gap was not observed in ARPES results. To this end, we suggest that experiments should focus on the high-resolution energy dispersion along the  $-K$  to  $\Gamma$  to  $K$  line and probe the symmetry-breaking without symmetrizing the ARPES data. Even in the presence of required surface magnetism, apparent symmetry-breaking exists only in selected energy windows where surface states are mainly contributed by the  $\text{MnBi}_2\text{Te}_4$  layer.

#### V. ACKNOWLEDGEMENTS

We thank Shuolong Yang for helpful discussions. H.T. thanks the support from the Dean of Faculty Fellowship at Weizmann Institute of Science. B.Y. acknowledges the financial support from the European Research Council (ERC Consolidator Grant, No. 815869) and the Israel Science Foundation (ISF No. 3520/20).

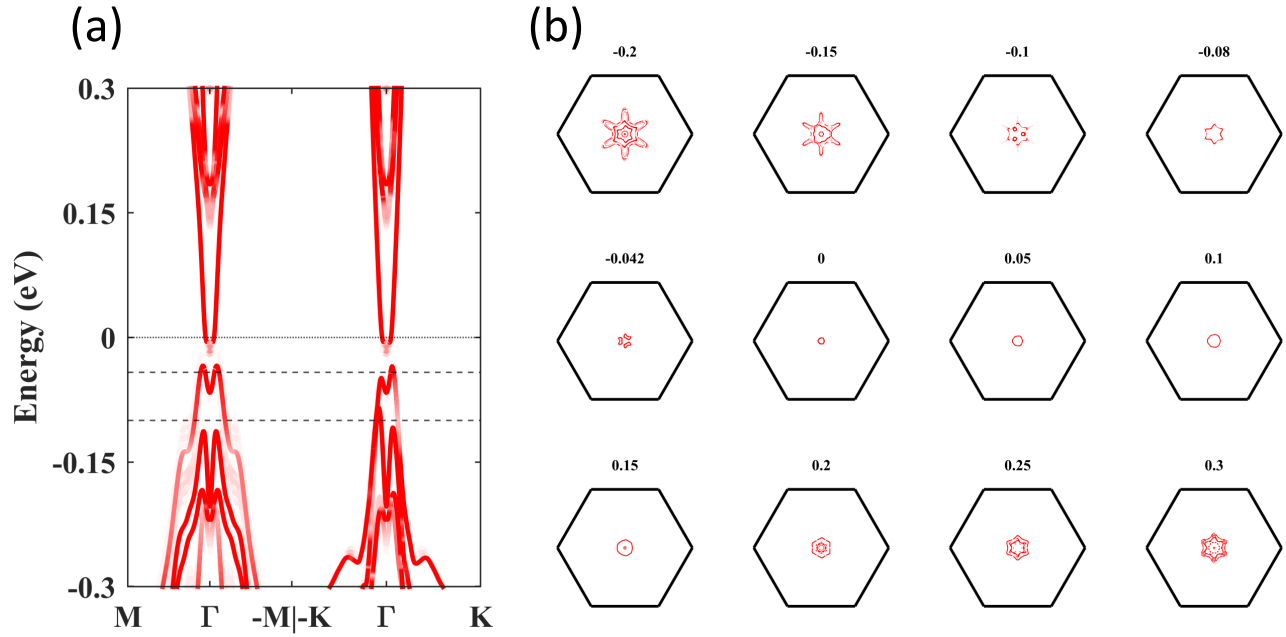


FIG. 3. Similar to Fig. 2 but for the  $\text{Bi}_2\text{Te}_3$ -terminated surface of  $\text{MnBi}_4\text{Te}_7$ : (a) surface states in red (the larger the weight of the surface the darker the red color) and (b) constant-energy contours at different energies. Similar to the  $\text{MnBi}_2\text{Te}_4$  surface in Fig. 2, the surface states and constant-energy contours indicate only  $C_{3v}$  symmetry of the surface states while the  $C_{6v}$  symmetry is well maintained at many energies, *e.g.* the experiment Fermi level. The most prominent symmetry breaking happens not only at the top of the surface valence bands ( $-0.042$  eV) but also at the energy of about  $-0.1$  eV, as indicated by the dashed lines in (a). The maximum of the bulk valence bands is set to energy zero.

- 
- [1] Yan Gong, Jingwen Guo, Jiaheng Li, Kejing Zhu, Menghan Liao, Xiaozhi Liu, Qinghua Zhang, Lin Gu, Lin Tang, Xiao Feng, Ding Zhang, Wei Li, Canli Song, Lili Wang, Pu Yu, Xi Chen, Yayu Wang, Hong Yao, Wenhui Duan, Yong Xu, Shou-Cheng Zhang, Xucun Ma, Qi-Kun Xue, and Ke He, “Experimental realization of an intrinsic magnetic topological insulator,” *Chin. Phys. Lett.* **36**, 076801 (2019).
- [2] M. M. Otrokov, I. I. Klimovskikh, H. Bentmann, D. Estyunin, A. Zeugner, Z. S. Aliev, S. Gaß, A. U. B. Wolter, A. V. Koroleva, A. M. Shikin, M. Blanco-Rey, M. Hoffmann, I. P. Rusinov, A. Yu. Vyazovskaya, S. V. Ere-meev, Yu. M. Koroteev, V. M. Kuznetsov, F. Freyse, J. Sánchez-Barriga, I. R. Amiraslanov, M. B. Babanly, N. T. Mamedov, N. A. Abdullayev, V. N. Zverev, A. Alfonsov, V. Kataev, B. Büchner, E. F. Schwier, S. Kumar, A. Kimura, L. Petaccia, G. Di Santo, R. C. Vidal, S. Schatz, K. Kißner, M. Ünzelmann, C. H. Min, Simon Moser, T. R. F. Peixoto, F. Reinert, A. Ernst, P. M. Echenique, A. Isaeva, and E. V. Chulkov, “Prediction and observation of an antiferromagnetic topological insulator,” *Nature* **576**, 416–422 (2019).
- [3] Jiaheng Li, Yang Li, Shiqiao Du, Zun Wang, Bing-Lin Gu, Shou-Cheng Zhang, Ke He, Wenhui Duan, and Yong Xu, “Intrinsic magnetic topological insulators in van der Waals layered  $\text{MnBi}_2\text{Te}_4$ -family materials,” *Sci. Adv.* **5**, eaaw5685 (2019).
- [4] Dongqin Zhang, Minji Shi, Tongshuai Zhu, Dingyu Xing, Haijun Zhang, and Jing Wang, “Topological Axion States in the Magnetic Insulator  $\text{MnBi}_2\text{Te}_4$  with the Quantized Magnetoelectric Effect,” *Phys. Rev. Lett.* **122**, 206401 (2019).
- [5] Cui-Zu Chang, Jinsong Zhang, Xiao Feng, Jie Shen, Zuocheng Zhang, Minghua Guo, Kang Li, Yunbo Ou, Pang Wei, Li-Li Wang, Zhong-Qing Ji, Yang Feng, Shuaihua Ji, Xi Chen, Jinfeng Jia, Xi Dai, Zhong Fang, Shou-Cheng Zhang, Ke He, Yayu Wang, Li Lu, Xu-Cun Ma, and Qi-Kun Xue, “Experimental observation of the quantum anomalous hall effect in a magnetic topological insulator,” *Science* **340**, 167–170 (2013).
- [6] Yujun Deng, Yijun Yu, Meng Zhu Shi, Zhongxun Guo, Zihan Xu, Jing Wang, Xian Hui Chen, and Yuanbo Zhang, “Quantum anomalous Hall effect in intrinsic magnetic topological insulator  $\text{MnBi}_2\text{Te}_4$ ,” *Science* **367**, 895–900 (2020).
- [7] Jun Ge, Yanzhao Liu, Jiaheng Li, Hao Li, Tianchuang Luo, Yang Wu, Yong Xu, and Jian Wang, “High- Chern-number and high-temperature quantum hall effect without Landau levels,” *National Science Review* **7**, 1280–1287 (2020).
- [8] Haiming Deng, Zhiyi Chen, Agnieszka Wołoś, Marcin Konczykowski, Kamil Sobczak, Joanna Sitnicka, Irina V. Fedorchenko, Jolanta Borysiuk, Tristan Heider, Łukasz Pluciński, Kyungwha Park, Alexandru B. Georgescu, Jennifer Cano, and Lia Krusin-Elbaum, “High-



- temperature quantum anomalous Hall regime in a  $\text{MnBi}_2\text{Te}_4/\text{Bi}_2\text{Te}_3$  superlattice,” *Nature Physics* **17**, 36–42 (2021).
- [9] Masataka Mogi, Minoru Kawamura, Atsushi Tsukazaki, Ryutaro Yoshimi, Kei S. Takahashi, Masashi Kawasaki, and Yoshinori Tokura, “Tailoring tricolor structure of magnetic topological insulator for robust axion insulator,” *Science Advances* **3**, eaao1669 (2017).
  - [10] Di Xiao, Jue Jiang, Jae-Ho Shin, Wenbo Wang, Fei Wang, Yi-Fan Zhao, Chaoxing Liu, Weida Wu, Moses H. W. Chan, Nitin Samarth, and Cui-Zu Chang, “Realization of the axion insulator state in quantum anomalous hall sandwich heterostructures,” *Phys. Rev. Lett.* **120**, 056801 (2018).
  - [11] Chang Liu, Yongchao Wang, Hao Li, Yang Wu, Yaixin Li, Jiaheng Li, Ke He, Yong Xu, Jinsong Zhang, and Yayu Wang, “Robust axion insulator and chern insulator phases in a two-dimensional antiferromagnetic topological insulator,” *Nature materials* **19**, 522–527 (2020).
  - [12] M. M. Otrokov, I. P. Rusinov, M. Blanco-Rey, M. Hoffmann, A. Yu. Vyazovskaya, S. V. Eremeev, A. Ernst, P. M. Echenique, A. Arnau, and E. V. Chulkov, “Unique Thickness-Dependent Properties of the van der Waals Interlayer Antiferromagnet  $\text{MnBi}_2\text{Te}_4$  Films,” *Phys. Rev. Lett.* **122**, 107202 (2019).
  - [13] Jiazhen Wu, Fucai Liu, Masato Sasase, Koichiro Ienaga, Yukiko Obata, Ryu Yukawa, Koji Horiba, Hiroshi Kumigashira, Satoshi Okuma, Takeshi Inoshita, and Hideo Hosono, “Natural van der waals heterostructural single crystals with both magnetic and topological properties,” *Science Advances* **5**, eaax9989 (2019).
  - [14] Shangjie Tian, Shunye Gao, Simin Nie, Yuting Qian, Chunsheng Gong, Yang Fu, Hang Li, Wenhui Fan, Peng Zhang, Takeshi Kondo, Shik Shin, Johan Adell, Hanna Fedderwitz, Hong Ding, Zhijun Wang, Tian Qian, and Hechang Lei, “Magnetic topological insulator  $\text{mnbi}_6\text{te}_{10}$  with a zero-field ferromagnetic state and gapped dirac surface states,” *Phys. Rev. B* **102**, 035144 (2020).
  - [15] Xiao-Ming Ma, Zhongjia Chen, Eike F. Schwier, Yang Zhang, Yu-Jie Hao, Shiv Kumar, Ruie Lu, Jifeng Shao, Yuanjun Jin, Meng Zeng, Xiang-Rui Liu, Zhanyang Hao, Ke Zhang, Wumiti Mansuer, Chunyao Song, Yuan Wang, Boyan Zhao, Cai Liu, Ke Deng, Jiawei Mei, Kenya Shimada, Yue Zhao, Xingjiang Zhou, Bing Shen, Wen Huang, Chang Liu, Hu Xu, and Chaoyu Chen, “Hybridization-induced gapped and gapless states on the surface of magnetic topological insulators,” *Phys. Rev. B* **102**, 245136 (2020).
  - [16] Haoyuan Zhong, Changhua Bao, Huan Wang, Jiaheng Li, Zichen Yin, Yong Xu, Wenhui Duan, Tian-Long Xia, and Shuyun Zhou, “Light-Tunable Surface State and Hybridization Gap in Magnetic Topological Insulator  $\text{MnBi}_8\text{Te}_{13}$ ,” *Nano Letters* **21**, 6080–6086 (2021).
  - [17] Xuefeng Wu, Jiayu Li, Xiao-Ming Ma, Yu Zhang, Yuntian Liu, Chun-Sheng Zhou, Jifeng Shao, Qiaoming Wang, Yu-Jie Hao, Yue Feng, Eike F. Schwier, Shiv Kumar, Hongyi Sun, Pengfei Liu, Kenya Shimada, Koji Miyamoto, Taichi Okuda, Kedong Wang, Maohai Xie, Chaoyu Chen, Qihang Liu, Chang Liu, and Yue Zhao, “Distinct Topological Surface States on the Two Terminations of  $\text{MnBi}_4\text{Te}_7$ ,” *Phys. Rev. X* **10**, 031013 (2020).
  - [18] Yu-Jie Hao, Pengfei Liu, Yue Feng, Xiao-Ming Ma, Eike F. Schwier, Masashi Arita, Shiv Kumar, Chaowei Hu, Rui’e Lu, Meng Zeng, Yuan Wang, Zhanyang Hao, Hong-Yi Sun, Ke Zhang, Jiawei Mei, Ni Ni, Liusuo Wu, Kenya Shimada, Chaoyu Chen, Qihang Liu, and Chang Liu, “Gapless Surface Dirac Cone in Antiferromagnetic Topological Insulator  $\text{MnBi}_2\text{Te}_4$ ,” *Phys. Rev. X* **9**, 041038 (2019).
  - [19] Hang Li, Shun-Ye Gao, Shao-Feng Duan, Yuan-Feng Xu, Ke-Jia Zhu, Shang-Jie Tian, Jia-Cheng Gao, Wen-Hui Fan, Zhi-Cheng Rao, Jie-Rui Huang, Jia-Jun Li, Da-Yu Yan, Zheng-Tai Liu, Wan-Ling Liu, Yao-Bo Huang, Yu-Liang Li, Yi Liu, Guo-Bin Zhang, Peng Zhang, Takeshi Kondo, Shik Shin, He-Chang Lei, You-Guo Shi, Wen-Tao Zhang, Hong-Ming Weng, Tian Qian, and Hong Ding, “Dirac Surface States in Intrinsic Magnetic Topological Insulators  $\text{EuSn}_2\text{As}_2$  and  $\text{MnBi}_{2n}\text{Te}_{3n+1}$ ,” *Phys. Rev. X* **9**, 041039 (2019).
  - [20] Y. J. Chen, L. X. Xu, J. H. Li, Y. W. Li, H. Y. Wang, C. F. Zhang, H. Li, Y. Wu, A. J. Liang, C. Chen, S. W. Jung, C. Cacho, Y. H. Mao, S. Liu, M. X. Wang, Y. F. Guo, Y. Xu, Z. K. Liu, L. X. Yang, and Y. L. Chen, “Topological Electronic Structure and Its Temperature Evolution in Antiferromagnetic Topological Insulator  $\text{MnBi}_2\text{Te}_4$ ,” *Phys. Rev. X* **9**, 041040 (2019).
  - [21] Raphael C. Vidal, Alexander Zeugner, Jorge I. Facio, Rajyavardhan Ray, M. Hossein Haghighi, Anja U. B. Wolter, Laura T. Corredor Bohorquez, Federico Cagliaris, Simon Moser, Tim Figgemeier, Thiago R. F. Peixoto, Hari Babu Vasili, Manuel Valvidares, Sungwon Jung, Cephise Cacho, Alexey Alfonsov, Kavita Mehlaawat, Vladislav Kataev, Christian Hess, Manuel Richter, Bernd Büchner, Jeroen van den Brink, Michael Ruck, Friedrich Reinert, Hendrik Bentmann, and Anna Isaeva, “Topological Electronic Structure and Intrinsic Magnetization in  $\text{MnBi}_4\text{Te}_7$ : A  $\text{Bi}_2\text{Te}_3$  Derivative with a Periodic Mn Sublattice,” *Phys. Rev. X* **9**, 041065 (2019).
  - [22] Przemyslaw Swatek, Yun Wu, Lin-Lin Wang, Kyungchan Lee, Benjamin Schrunk, Jiaqiang Yan, and Adam Kaminski, “Gapless Dirac surface states in the antiferromagnetic topological insulator  $\text{MnBi}_2\text{Te}_4$ ,” *Phys. Rev. B* **101**, 161109 (2020).
  - [23] Lixuan Xu, Yuanhao Mao, Hongyuan Wang, Jiaheng Li, Yujie Chen, Yunyouyou Xia, Yiwei Li, Ding Pei, Jing Zhang, Huijun Zheng, Kui Huang, Chaofan Zhang, Shengtao Cui, Aiji Liang, Wei Xia, Hao Su, Sungwon Jung, Cephise Cacho, Meixiao Wang, Gang Li, Yong Xu, Yanfeng Guo, Lexian Yang, Zhongkai Liu, Yulin Chen, and Mianheng Jiang, “Persistent surface states with diminishing gap in  $\text{MnBi}_2\text{Te}_4/\text{Bi}_2\text{Te}_3$  superlattice antiferromagnetic topological insulator,” *Science Bulletin* **65**, 2086–2093 (2020).
  - [24] Chaowei Hu, Kyle N. Gordon, Pengfei Liu, Jinyu Liu, Xiaoqing Zhou, Peipei Hao, Dushyant Narayan, Eve Emmanouilidou, Hongyi Sun, Yuntian Liu, Harlan Brawer, Arthur P. Ramirez, Lei Ding, Huibo Cao, Qihang Liu, Dan Dessau, and Ni Ni, “A van der waals antiferromagnetic topological insulator with weak interlayer magnetic coupling,” *Nature communications* **11**, 97 (2020).
  - [25] Yong Hu, Lixuan Xu, Mengzhu Shi, Aiyun Luo, Shut-ing Peng, Z. Y. Wang, J. J. Ying, T. Wu, Z. K. Liu, C. F. Zhang, Y. L. Chen, G. Xu, X.-H. Chen, and J.-F. He, “Universal gapless Dirac cone and tunable topological states in  $(\text{MnBi}_2\text{Te}_4)_m(\text{Bi}_2\text{Te}_3)_n$  heterostructures,” *Phys. Rev. B* **101**, 161113 (2020).
  - [26] Na Hyun Jo, Lin-Lin Wang, Robert-Jan Slager, Jiaqiang Yan, Yun Wu, Kyungchan Lee, Benjamin Schrunk,

- Ashvin Vishwanath, and Adam Kaminski, “Intrinsic axion insulating behavior in antiferromagnetic  $\text{MnBi}_6\text{Te}_{10}$ ,” *Phys. Rev. B* **102**, 045130 (2020).
- [27] R. C. Vidal, H. Bentmann, J. I. Facio, T. Heider, P. Kagerer, C. I. Fornari, T. R. F. Peixoto, T. Figge-meier, S. Jung, C. Cacho, B. Büchner, J. van den Brink, C. M. Schneider, L. Plucinski, E. F. Schwier, K. Shimada, M. Richter, A. Isaeva, and F. Reinert, “Orbital Complexity in Intrinsic Magnetic Topological Insulators  $\text{MnBi}_4\text{Te}_7$  and  $\text{MnBi}_6\text{Te}_{10}$ ,” *Phys. Rev. Lett.* **126**, 176403 (2021).
- [28] Yaohua Liu, Lin-Lin Wang, Qiang Zheng, Zengle Huang, Xiaoping Wang, Miaofang Chi, Yan Wu, Bryan C. Chakoumakos, Michael A. McGuire, Brian C. Sales, Weida Wu, and Jiaqiang Yan, “Site Mixing for Engineering Magnetic Topological Insulators,” *Phys. Rev. X* **11**, 021033 (2021).
- [29] Yonghao Yuan, Xintong Wang, Hao Li, Jiaheng Li, Yu Ji, Zhenqi Hao, Yang Wu, Ke He, Yayu Wang, Yong Xu, Wenhui Duan, Wei Li, and Qi-Kun Xue, “Electronic States and Magnetic Response of  $\text{MnBi}_2\text{Te}_4$  by Scanning Tunneling Microscopy and Spectroscopy,” *Nano Letters* **20**, 3271–3277 (2020).
- [30] Fuchen Hou, Qiushi Yao, Chun-Sheng Zhou, Xiao-Ming Ma, Mengjiao Han, Yu-Jie Hao, Xuefeng Wu, Yu Zhang, Hongyi Sun, Chang Liu, Yue Zhao, Qihang Liu, and Junhao Lin, “Te-Vacancy-Induced Surface Collapse and Reconstruction in Antiferromagnetic Topological Insulator  $\text{MnBi}_2\text{Te}_4$ ,” *ACS Nano* **14**, 11262–11272 (2020).
- [31] Alexander M Shikin, DA Estyunin, Ilya I Klimovskikh, SO Filnov, EF Schwier, S Kumar, Koji Miyamoto, Taichi Okuda, A Kimura, K Kuroda, et al., “Nature of the Dirac gap modulation and surface magnetic interaction in axion antiferromagnetic topological insulator  $\text{MnBi}_2\text{Te}_4$ ,” *Scientific Reports* **10**, 1–13 (2020).
- [32] A. M. Shikin, D. A. Estyunin, N. L. Zaitsev, D. Glazkova, I. I. Klimovskikh, S. O. Filnov, A. G. Rybkin, E. F. Schwier, S. Kumar, A. Kimura, N. Mamedov, Z. Aliev, M. B. Babanly, K. Kokh, O. E. Tereshchenko, M. M. Otrokov, E. V. Chulkov, K. A. Zvezdin, and A. K. Zvezdin, “Sample-dependent Dirac-point gap in  $\text{MnBi}_2\text{Te}_4$  and its response to applied surface charge: A combined photoemission and ab initio study,” *Phys. Rev. B* **104**, 115168 (2021).
- [33] Jiaqiang Yan, “The elusive quantum anomalous Hall effect in  $\text{MnBi}_2\text{Te}_4$ : a materials perspective,” *arXiv:2112.09070* (2021).
- [34] M. Garnica, M. M. Otrokov, P. Casado Aguilar, I. I. Klimovskikh, D. Estyunin, Z. S. Aliev, I. R. Amiraslanov, N. A. Abdullayev, V. N. Zverev, M. B. Babanly, N. T. Mamedov, A. M. Shikin, A. Arnau, A. L. Vazquez de Parga, E. V. Chulkov, and R. Miranda, “Native point defects and their implications for the Dirac point gap at  $\text{MnBi}_2\text{Te}_4$  (0001),” *npj Quantum Materials* **7**, 1–9 (2022).
- [35] Ilya I. Klimovskikh, Mikhail M. Otrokov, Dmitry Estyunin, Sergey V. Ereemeev, Sergey O. Filnov, Alexandra Koroleva, Eugene Shevchenko, Vladimir Voroshnin, Artem G. Rybkin, Igor P. Rusinov, Maria Blanco-Rey, Martin Hoffmann, Ziya S. Aliev, Mahammad B. Babanly, Imamaddin R. Amiraslanov, Nadir A. Abdullayev, Vladimir N. Zverev, Akio Kimura, Oleg E. Tereshchenko, Konstantin A. Kokh, Luca Petaccia, Giovanni Di Santo, Arthur Ernst, Pedro M. Echenique, Nazim T. Mamedov, Alexander M. Shikin, and Eugene V. Chulkov, “Tunable 3D/2D magnetism in the  $(\text{MnBi}_2\text{Te}_4)(\text{Bi}_2\text{Te}_3)_m$  topological insulators family,” *npj Quantum Materials* **5**, 54 (2020).
- [36] Chaowei Hu, Lei Ding, Kyle N. Gordon, Barun Ghosh, Hung-Ju Tien, Haoxiang Li, A. Garrison Linn, Shang-Wei Lien, Cheng-Yi Huang, Scott Mackey, Jinyu Liu, P. V. Sreenivasa Reddy, Bahadur Singh, Amit Agarwal, Arun Bansil, Miao Song, Dongsheng Li, Su-Yang Xu, Hsin Lin, Huibo Cao, Tay-Rong Chang, Dan Dessau, and Ni Ni, “Realization of an intrinsic ferromagnetic topological state in  $\text{MnBi}_8\text{Te}_{13}$ ,” *Science Advances* **6**, eaba4275 (2020).
- [37] Jiazhen Wu, Fucui Liu, Can Liu, Yong Wang, Changcun Li, Yangfan Lu, Satoru Matsuishi, and Hideo Hosono, “Toward 2D Magnets in the  $(\text{MnBi}_2\text{Te}_4)(\text{Bi}_2\text{Te}_3)_n$  Bulk Crystal,” *Advanced Materials* **32**, 2001815 (2020).
- [38] Paul M. Sass, Jinwoong Kim, David Vanderbilt, Jiaqiang Yan, and Weida Wu, “Robust A-Type Order and Spin-Flop Transition on the Surface of the Antiferromagnetic Topological Insulator  $\text{MnBi}_2\text{Te}_4$ ,” *Phys. Rev. Lett.* **125**, 037201 (2020).
- [39] D. Nevola, H. X. Li, J.-Q. Yan, R. G. Moore, H.-N. Lee, H. Miao, and P. D. Johnson, “Coexistence of Surface Ferromagnetism and a Gapless Topological State in  $\text{MnBi}_2\text{Te}_4$ ,” *Phys. Rev. Lett.* **125**, 117205 (2020).
- [40] Enke Liu, Yan Sun, Nitesh Kumar, Lukas Muechler, Aili Sun, Lin Jiao, Shuo-Ying Yang, Defa Liu, Aiji Liang, Qiunan Xu, et al., “Giant anomalous hall effect in a ferromagnetic kagome-lattice semimetal,” *Nature physics* **14**, 1125–1131 (2018).
- [41] D. F. Liu, A. J. Liang, E. K. Liu, Q. N. Xu, Y. W. Li, C. Chen, D. Pei, W. J. Shi, S. K. Mo, P. Dudin, T. Kim, C. Cacho, G. Li, Y. Sun, L. X. Yang, Z. K. Liu, S. S. P. Parkin, C. Felser, and Y. L. Chen, “Magnetic weyl semimetal phase in a kagomé crystal,” *Science* **365**, 1282–1285 (2019).
- [42] Noam Morali, Rajib Batabyal, Pranab Kumar Nag, Enke Liu, Qiunan Xu, Yan Sun, Binghai Yan, Claudia Felser, Nurit Avraham, and Haim Beidenkopf, “Fermi-arc diversity on surface terminations of the magnetic Weyl semimetal  $\text{Co}_3\text{Sn}_2\text{S}_2$ ,” *Science* **365**, 1286–1291 (2019).
- [43] Georg Kresse and Jürgen Furthmüller, “Efficiency of ab-initio total energy calculations for metals and semiconductors using a plane-wave basis set,” *Comput. Mater. Sci.* **6**, 15–50 (1996).
- [44] G. Kresse and J. Furthmüller, “Efficient iterative schemes for ab initio total-energy calculations using a plane-wave basis set,” *Phys. Rev. B* **54**, 11169 (1996).
- [45] John P. Perdew, Kieron Burke, and Matthias Ernzerhof, “Generalized gradient approximation made simple,” *Phys. Rev. Lett.* **77**, 3865 (1996).
- [46] Stefan Grimme, Jens Antony, Stephan Ehrlich, and Helge Krieg, “A consistent and accurate ab initio parametrization of density functional dispersion correction (DFT-D) for the 94 elements H-Pu,” *J. Chem. Phys.* **132**, 154104 (2010).
- [47] Nicola Marzari and David Vanderbilt, “Maximally localized generalized wannier functions for composite energy bands,” *Phys. Rev. B* **56**, 12847–12865 (1997).
- [48] Arash A. Mostofi, Jonathan R. Yates, Young-Su Lee, Ivo Souza, David Vanderbilt, and Nicola Marzari, “wannier90: A tool for obtaining maximally-localised wannier functions,” *Computer Physics Communications* **178**,

- 685–699 (2008).
- [49] Hengxin Tan and Binghai Yan, “Facet dependent surface energy gap on magnetic topological insulators,” *Phys. Rev. B* **105**, 165130 (2022).
- [50] Qiunan Xu, Enke Liu, Wujun Shi, Lukas Muechler, Jacob Gayles, Claudia Felser, and Yan Sun, “Topological surface Fermi arcs in the magnetic Weyl semimetal  $\text{Co}_3\text{Sn}_2\text{S}_2$ ,” *Phys. Rev. B* **97**, 235416 (2018).